An intracellular membrane junction consisting of flagellum adhesion glycoproteins links flagellum biogenesis to cell morphogenesis in *Trypanosoma brucei*

Stella Y. Sun, Chao Wang, Y. Adam Yuan and Cynthia Y. He*

Department of Biological Sciences, NUS Centre for BioImaging Sciences, National University of Singapore, Singapore

*Author for correspondence (dbshyc@nus.edu.sg)

Accepted 22 October 2012
Journal of Cell Science 126, 520–531

doi: 10.1242/jcs.113621

Summary

African trypanosomes have a single, membrane-bounded flagellum that is attached to the cell cortex by membrane adhesion proteins and an intracellular flagellum attachment zone (FAZ) complex. The coordinated assembly of flagellum and FAZ, during the cell cycle and the life cycle development, plays a pivotal role in organelle positioning, cell division and cell morphogenesis. To understand how the flagellum and FAZ assembly are coordinated, we examined the domain organization of the flagellum adhesion protein 1 (FLA1), a glycosylated, transmembrane protein essential for flagellum attachment and cell division. By immunoprecipitation of a FLA1-truncation mutant that mislocalized to the flagellum, a novel FLA1-binding protein (FLA1BP) was identified in procyclic *Trypanosoma brucei*. The interaction between FLA1 on the cell membrane and FLA1BP on the flagellum membrane acts like a molecular zipper, joining flagellum membrane to cell membrane and linking flagellum biogenesis to FAZ elongation. By coordinating flagellum and FAZ assembly during the cell cycle, morphology information is transmitted from the flagellum to the cell body.

Key words: Flagellum, Flagellum attachment zone (FAZ), Flagellum adhesion proteins, Cell morphogenesis, *Trypanosoma brucei*

Introduction

Kinetoplastid parasites including *Trypanosoma brucei*, *Trypanosoma cruzi* and *Leishmania* spp. are important human and veterinary pathogens that still remain a threat to global health and productivity (Mathers et al., 2007). These single-cellular organisms are characterized by the presence of a single flagellum, which is important for normal cell motility, cell division, immune evasion and host-parasite interactions (Broadhead et al., 2006; Engstler et al., 2007; Oberholzer et al., 2011; Ralston et al., 2006). Like many eukaryotic organelles, size regulation has been observed for the flagellum in trypanosomatid parasites and the control of the flagellum length is important for their parasitic life style (Gluenz et al., 2010). In *Leishmania*, the flagellum undergoes tight regulation so that a long flagellum is present in the extracellular, motile parasite and only a small residual flagellum is present in the intracellular, immotile amastigote cells. Flagellum length also varies during *T. brucei* life cycle development and its length is tightly coupled to the FAZ length and cell body length (Rotureau et al., 2011; Sharma et al., 2008).

In procyclic form *T. brucei*, which proliferates in the midgut of tsetse flies, each parasite cell contains a single flagellum seeded by the basal bodies that are physically attached to the kinetoplast (mitochondrial DNA) (Ogbadoyi et al., 2003). During the cell cycle, a new flagellum is assembled posterior to the existing flagellum, with its distal end attached to the old flagellum through the flagella connector (FC). As cell cycle progresses, little growth occurs at the old flagellum, whereas the new flagellum, guided by the FC, elongates along the old flagellum, duplicating the exact same length and helical pattern as the old structure (Moreira-Leite et al., 2001). Elongation of the new flagellum is accompanied with the assembly of a new flagellum attachment zone (FAZ) (Kohl et al., 1999), a mostly intracellular structure containing protein filament, microtubules and associated endoplasmic reticulum (Sherwin and Gull, 1989). The coordinated flagellum/FAZ assembly is required for the highly ordered segregation of single-copy organelles including the kinetoplast and the associated basal bodies (Absalon et al., 2007; Vaughan, 2010). It also plays an important role in cell morphogenesis, by regulating the organization of the subpellicular microtubules that subtends the plasma membrane (Kohl et al., 2003; Sherwin and Gull, 1989; Zhou et al., 2011). However, the molecular mechanism of the coordinated flagellum/FAZ assembly remains unknown.

In trypanosomes, the membrane-bound flagellum adheres to the cell body via membrane-associated glycoproteins. The first such molecule characterized was GP72, a stage-specific, glycosylated membrane protein in *T. cruzi* (Cooper et al., 1991). GP72 was readily detected along the flagellum adjacent to the adhesion region using indirect immunofluorescence on live, non-permeabilized parasites (Haynes et al., 1996). While GP72 null mutants are viable, *T. cruzi* cells without GP72 contain detached flagella and drastically changed cell morphology (Cooper et al., 1993). FLA1, the *T. brucei* homolog to GP72, is an essential

protein, functioning in both flagellum attachment and cell division, likely through regulation of FAZ assembly (LaCount et al., 2002; Nozaki et al., 1996). As a transmembrane protein with a large extracellular domain and a 16-amino-acid cytoplasmic tail (LaCount et al., 2002), how FLA1 mediates flagellum membrane adhesion is not yet clear.

In this study, we performed domain analysis of the FLA1 protein in procyclic *T. brucei* where the function of FLA1 is best characterized. While the 16-amino-acid tail is required for correct targeting of FLA1 to the FAZ, the extracellular domain is important for flagellum attachment through its interaction with a novel FLA1-interacting protein, FLA1BP. The specific interaction between FLA1BP on the flagellum and FLA1 on the cell body, provides the molecular basis for the membrane–membrane adhesion between flagellum and cell. This unique intracellular membrane junction facilitates the coordinated assembly of flagellum and FAZ, and mediates flagellum regulation of cell morphogenesis.

Results

Either extracellular or intracellular domains of FLA1, together with the transmembrane domain, can mediate protein targeting to the flagellum attachment region

FLA1 is a surface glycoprotein dually required for flagellum attachment and cytokinesis (LaCount et al., 2002). It contains an N-terminal signal peptide, followed by a glycosylated, extracellular domain, a transmembrane domain and a C-terminal 16-amino-acid tail (Fig. 1A). The extracellular domain was predicted to contain NHL repeats, which have been found in various proteins including growth regulators and membrane

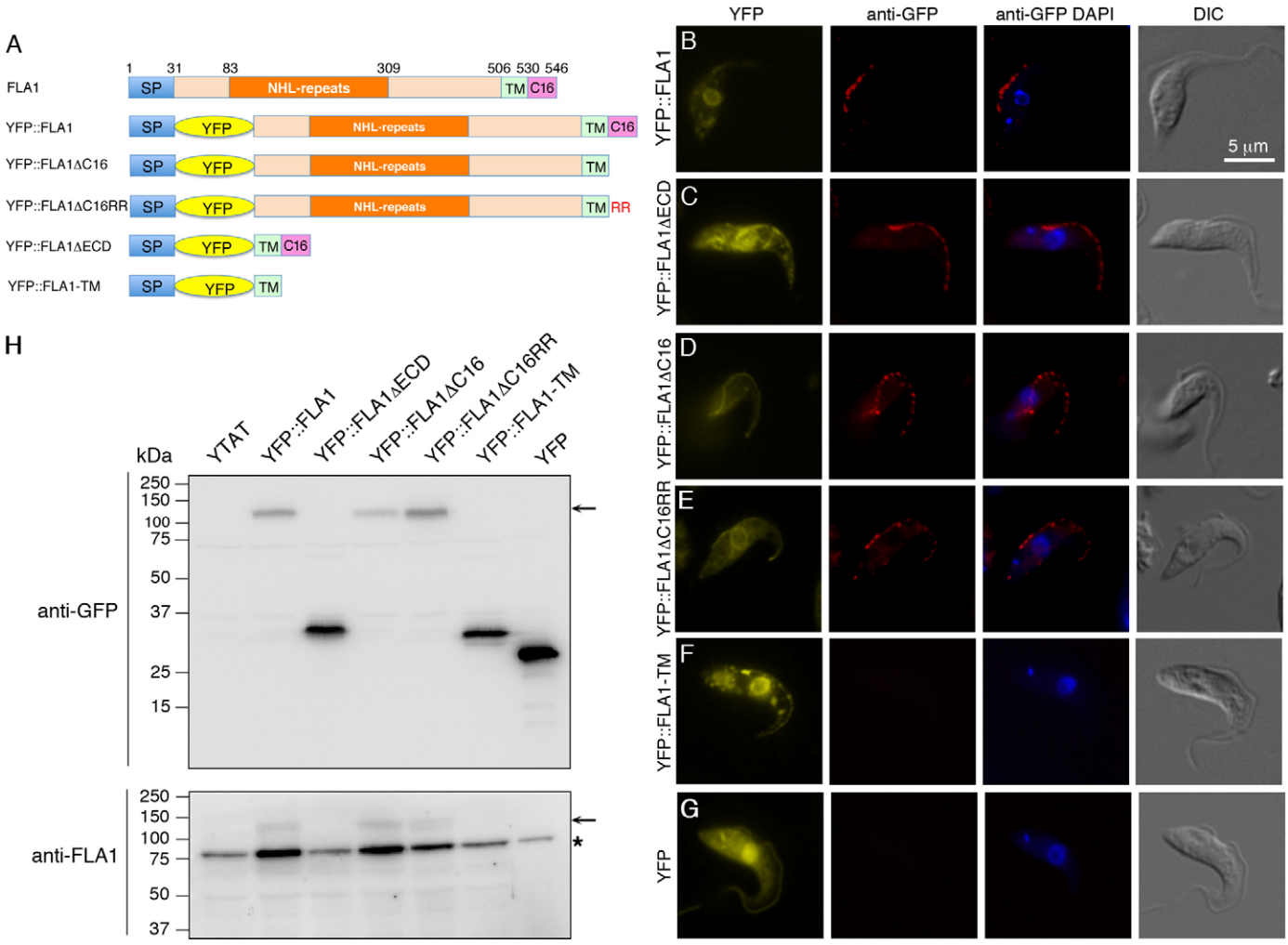

Fig. 1. Domain organization of FLA1. (**A**) A schematic view of the domain organization of FLA1 and the truncation mutants. FLA1 contains a signal peptide (SP) at the N-terminus, an NHL-repeat-containing extracellular domain (ECD), and a transmembrane domain (TM) followed by a C-terminal 16-amino-acid tail (C16). Numbers indicate the amino acid residues. (**B–G**) Cell surface immunofluorescence analysis of YFP::FLA1 and its truncation mutants. Live cells stably expressing YFP::FLA1 (B), YFP::FLA1ΔECD (C), YFP::FLA1ΔC16 (D), YFP::FLA1ΔC16RR (E), YFP::FLA1-TM (F) or YFP alone (G) were surface immunolabeled with anti-GFP. Direct YFP fluorescence (yellow) reflects the overall cellular distribution of each YFP reporter, whereas indirect anti-GFP labeling (red) reveals YFP reporter distribution at the cell surface. All images were acquired and processed using the same conditions. (**H**) Lysates of cells stably expressing YFP::FLA1, YFP::FLA1ΔECD, YFP::FLA1ΔC16, YFP::FLA1ΔC16RR, YFP::FLA1-TM or YFP alone were fractionated by SDS-PAGE and immunoblotted with anti-GFP or anti-FLA1. The asterisk marks endogenous FLA1 protein and arrows mark YFP::FLA1, YFP::FLA1ΔC16 or YFP::FLA1ΔC16RR that contained the extracellular domain against which anti-FLA1 was raised. Note that the expression of YFP::FLA1, YFP::FLA1ΔC16 or YFP::FLA1ΔC16RR was lower than that of the endogenous FLA1, consistent with their relatively weak YFP intensity shown in B, D and E.

receptors and have been shown to be required for protein–protein interactions (Edwards et al., 2003; Slack and Ruvkun, 1998). Previous immunofluorescence analyses showed that FLA1, like GP72, was present along the flagellum adhesion region (Haynes et al., 1996; Nozaki et al., 1996). But it was not clear whether FLA1 (or GP72) was associated with the cell membrane or the flagellum membrane or both. Being the only flagellum adhesion protein characterized in *T. brucei* thus far, it was also not clear how FLA1 mediated the flagellum/cell membrane adhesion.

To examine the precise localization of FLA1 and the targeting requirements of this protein, various YFP fusions were constructed and stably overexpressed in procyclic *T. brucei* (Fig. 1). The localization of YFP-tagged FLA1 mutants was then monitored in non-permeabilized cells by direct YFP fluorescence or indirect immunofluorescence using anti-GFP (Fig. 1B–G). Whereas direct YFP fluorescence reflected the distribution of YFP reporters all over the cell, anti-GFP labeling of intact cells allowed specific detection of YFP reporters at cell surface. All FLA1 mutants, with YFP inserted immediately after the signal peptide, were found in reticulated structures throughout the parasite cell that overlapped with the endoplasmic reticulum (data not shown). This observation was consistent with the presence of the N-terminal signal peptide in FLA1 that allowed its entry into the secretory pathway. The strong YFP signal observed in the endomembrane system may also be due to YFP overexpression (Fig. 1H) or poor folding in these cells. Anti-GFP probing of non-permeabilized YFP::FLA1 cells specifically labeled along the flagellum attachment region (Fig. 1B), confirming the exclusive presence of the YFP reporter extracellularly at the flagellum attachment region. This was consistent with previous reports on FLA1 localization and membrane topology in *T. brucei* (LaCount et al., 2002; Nozaki et al., 1996). Similarly, HA-tagged GP72 was also found along the flagellum when live, non-permeabilized cells were probed with anti-HA (Haynes et al., 1996). Interestingly, FLA1 truncation mutants lacking the extracellular domain (YFP::FLA1ΔECD) or the C-terminal 16-amino-acid tail (YFP::FLA1ΔC16 and YFP::FLA1ΔC16RR, in which two arginine residues were inserted immediately after the transmembrane domain as stop transfer signal), could all be incorporated into the flagellum attachment region (Fig. 1C–E). YFP fusion to the transmembrane domain only (YFP::FLA1–TM) and YFP reporter alone, however, were both readily detected intracellularly but showed no specific targeting to the flagellum adhesion region (Fig. 1F,G). The extracellular accessibility of the YFP reporters was further evaluated by surface biotinylation assays (supplementary material Fig. S1). Whereas YFP::FLA1, YFP::FLA1ΔECD, YFP::FLA1ΔC16 and YFP::FLA1ΔC16RR could all be biotinylated and affinity purified with streptavidin beads, YFP::FLA1-TM and YFP alone could not, verifying the results of the immunofluorescence assays. These results suggested that either the extracellular domain or the C-terminal 16-amino-acid tail of FLA1, together with the transmembrane domain, could mediate protein targeting to the flagellum adhesion region.

Due to the flagellum attachment along the cell body, we reasoned that the precise localization of the FLA1 mutants could only be distinguished if the FLA1 mutants were expressed in cells with flagellum detached from the cell body. To achieve this, FLA1 cDNA with scrambled coding sequence (supplementary material Fig. S3) was synthesized and used as template for the construction of RNAi-resistant FLA1 mutants, which were then expressed in FLA1-RNAi cells (Fig. 2). The tetracycline-inducible depletion of

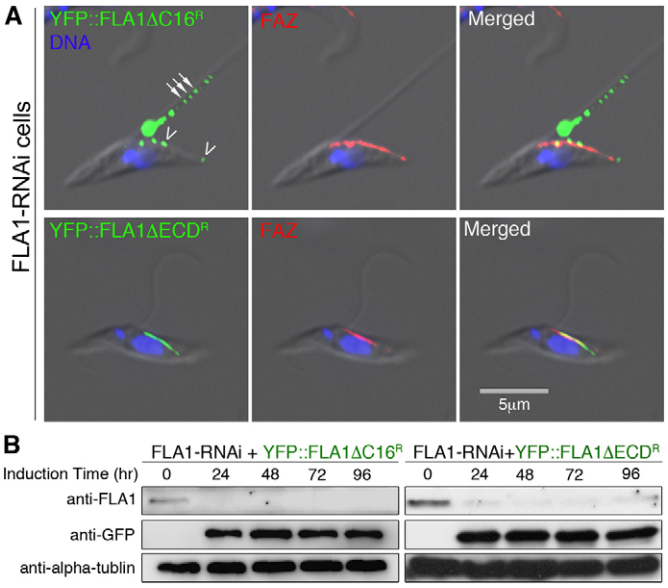

Fig. 2. The ECD and the C16 in FLA1 each mediate specific targeting to the flagellum and the FAZ region. (**A**) RNAi-resistant FLA1 truncation mutants were inducibly expressed in cells induced for FLA1-RNAi, which led to flagellum detachment from the cell body. Cells were fixed with 4% PFA for 5 minutes and cold methanol for another 5 minutes, blocked with 3% BSA in PBS and then labeled with anti-GFP (green), L3B2 for FAZ (red) and DAPI for DNA (blue). Whereas YFP::FLA1ΔC16^{R} (lacking the cytoplasmic tail) targeted primarily to the detached flagellum in a dotted pattern (arrows), a few scattered dots were found on the side of the cell body (arrowheads). In contrast, YFP::FLA1ΔECD^{R} (lacking the extracellular domain) localized exclusively on the cell body side along the FAZ. (**B**) The inducible depletion of endogenous FLA1 and the inducible expression of YFP::FLA1ΔC16^{R} and YFP::FLA1ΔECD^{R} were monitored by immunoblotting with anti-FLA1 and anti-GFP every 24 hours over the course of induction. α-Tubulin was used as loading control.

endogenous FLA1 and tetracycline-inducible expression of RNAi-resistant, YFP-tagged FLA1 truncation mutants were monitored by immunoblots using a monoclonal antibody against FLA1 (Nozaki et al., 1996) and anti-GFP, respectively (Fig. 2B). Consistent with previously observed (LaCount et al., 2002), upon the addition of tetracycline to induce FLA1-RNAi, the endogenous FLA1 was depleted (Fig. 2B), leading to flagellum detachment from the cell body (Fig. 2A). In these cells, the RNAi-resistant YFP::FLA1ΔECD^{R} localized exclusively to the cell bodies in a distinct, continuous line overlapping with the FAZ filament marked with L3B2 antibody (Kohl et al., 1999). YFP::FLA1ΔC16^{R}, on the other hand, localized mainly in punctate structures along the detached flagellum. Some scattered labeling of YFP::FLA1ΔC16^{R} was also found on the cell body side, aligning with the L3B2-labeled FAZ (Fig. 2A). There may be other explanations for these observations, but the simplest interpretation of these results is that the C-terminal 16 amino acids may be required for anchoring to the cell body along the FAZ, and the extracellular domain may interact specifically with a flagellum membrane protein, thus mislocalizing YFP::FLA1ΔC16^{R} to the flagellum in punctate dots.

Identification of an FLA1-interacting protein, FLA1BP

An co-immunoprecipitation approach was employed to identify the hypothetic, FLA1-binding protein on the flagellum membrane.

As outlined in Fig. 3A, FLA1-RNAi cells expressing YFP::FLA1-ΔC16^R were biotinylated to label all surface proteins. After cell lysis with sonication and detergent extraction, centrifugation-cleared cell lysates were used for co-immunoprecipitation with anti-GFP followed by affinity purification with streptavidin-coated beads. Proteins eluted from the streptavidin beads were then analyzed by silver staining and immunoblots (Fig. 3B–D). Two bands were specifically detected in YFP::FLA1ΔC16^R cells relative to cells expressing YFP only, which was used as a negative control (Fig. 3B). One was a ~110 kDa protein that was labeled with both anti-GFP and anti-biotin (Fig. 3C,D), representing the YFP::FLA1ΔC16^R protein and this was confirmed by mass spectrometry analysis. The other was an ~80 kDa band which could be detected only by anti-biotin, but not by anti-GFP, possibly representing a FLA1-binding protein. Mass spectrometry identified a single, previously uncharacterized protein (encoded by two identical genes Tb927.8.4050 and Tb927.8.4100; see Table 1), which we named FLA1BP. Bioinformatic analyses of FLA1BP revealed a domain organization strikingly similar to that of FLA1, despite the lack of sequence similarity between these two proteins. Following a signal peptide near the N-terminus, FLA1BP possessed an NHL-repeat-containing domain, followed by a transmembrane domain and a C-terminal 40-amino-acid tail (Fig. 4A). The interaction between FLA1 and FLA1BP was also verified by reverse co-immunoprecipitation, where FLA1 was shown to co-precipitate with YFP::FLA1BP (supplementary material Fig. S4).

FLA1BP is a flagellum protein required for membrane adhesion, but is not essential for procyclic *T. brucei* survival in culture

YFP::FLA1BP was constructed by inserting the YFP reporter immediately after the N-terminal signal peptide and before the NHL repeats (Fig. 4A). Localization of YFP::FLA1BP was then evaluated by YFP fluorescence or anti-GFP labeling of non-permeabilized cells induced for FLA1-RNAi or not. In un-induced control cells, YFP::FLA1BP was found all over the cell by direct YFP fluorescence, similar to YFP::FLA1 (Fig. 4B). By surface labeling with anti-GFP, YFP::FLA1BP localized exclusively along the flagellum attachment region (Fig. 4B). This result also indicated that the YFP moiety in YFP::FLA1BP was accessible extracellularly, supporting that the region between the signal peptide and the transmembrane domain, including the NHL repeats, was also extracellular, just like FLA1.

Interestingly, in FLA1-RNAi cells, YFP::FLA1BP was detected only along the detached flagellum in a dotted pattern by anti-GFP (Fig. 4B). This localization pattern did not require the extracellular domain of FLA1BP, as YFP::FLA1BPΔECD targeted properly to the detached flagellum, in a dotted pattern similar to that observed for YFP::FLA1BP (Fig. 4D).

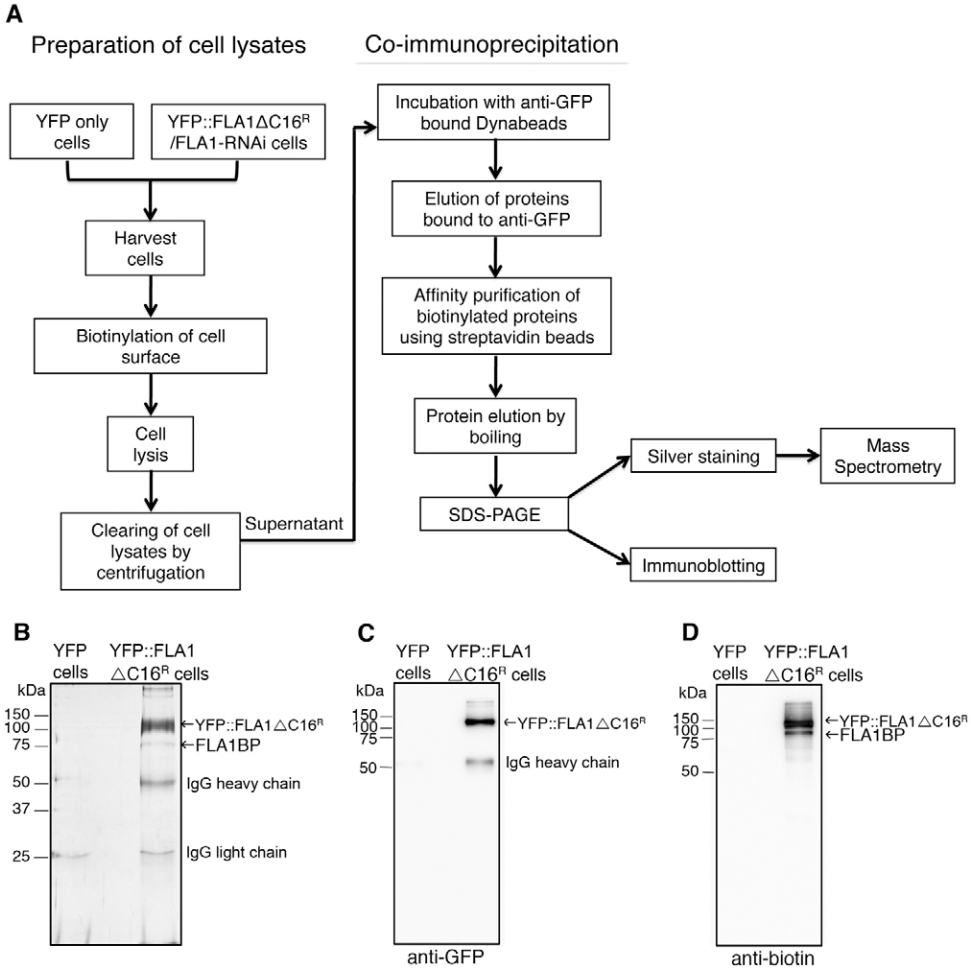

Fig. 3. Identification of a FLA1 binding protein, FLA1BP, by sequential co-immunoprecipitation (co-IP) and affinity purifications. (**A**) Flow chart of the purification procedure to identify biotinylated, YFP::FLA1ΔC16^R binding protein FLA1BP (see Materials and Methods for details). Cell expressing YFP only were used as a control. (**B–D**) Silver staining and immunoblots of the co-IP products. After the sequential co-IP/affinity purification process, two specific protein bands were detected by silver staining (B) and both proteins were biotinylated as shown by anti-biotin labeling (D). The higher molecular weight band was also recognized by anti-GFP (C) and therefore represented YFP::FLA1ΔC16^R. Mass spectrometry analysis of the lower molecular weight band (B, red arrow) identified a previously uncharacterized, putative FLA1-binding protein named as FLA1BP.

Table 1. NHL-repeat-containing transmembrane proteins in *T. brucei*

Gene annotation	Gene IDs	Primary sequence identity/similarity			mRNA expression profile	Orthologs	
		FLA1	FLA2	FLA1BP		*Leishmania* spp.	*T. cruzi*
FLA1	Tb927.8.4010	100%	60.6%/72.8%	X	Procyclic	Yes	Yes
FLA2	Tb927.8.4060	58%/71.1%	100%	X	BSF	Yes	Yes
FLA3	Tb927.8.4110	60.6%/72.8%	97.5%/98.3%	X	BSF	Yes	Yes
FLA1BP	Tb927.8.4050; Tb927.8.4100	X	X	100%	Procyclic	Yes	Yes
Hypothetical	Tb927.5.4570; Tb927.5.4580	X	X	40.5%/54.9%	BSF	No	No
Hypothetical	Tb927.10.6180	X	X	X	Both	Yes	Yes

X denotes lack of significant sequence similarity.

The dotted labeling pattern of FLA1BP along the flagellum suggested a possible anchoring of FLA1BP to flagellum skeleton, which contains a 9+2 microtubular axoneme and a paraflagellar rod (PFR) lattice, both with regular structural repeats. Neither the localization of YFP::FLA1BP to the flagellum, nor its dotted pattern was affected in cells lacking PFR that were additionally depleted of PFR2 (Fig. 4E) (Bastin et al., 1998), suggesting that FLA1BP may interact directly with flagellum axoneme.

The presence of FLA1BP on the flagellum and its interaction with FLA1 suggested that their interaction could mediate the flagellum–cell adhesion observed in *T. brucei*. To test this, FLA1BP was depleted using inducible RNAi. Efficient RNAi was verified by reverse transcriptase (RT)-PCR and immunoblots (Fig. 5B,C). As specific antibody against FLA1BP was not available, YFP::FLA1BP was stably expressed in FLA1BP-RNAi cells and its depletion upon tetracycline induction was monitored

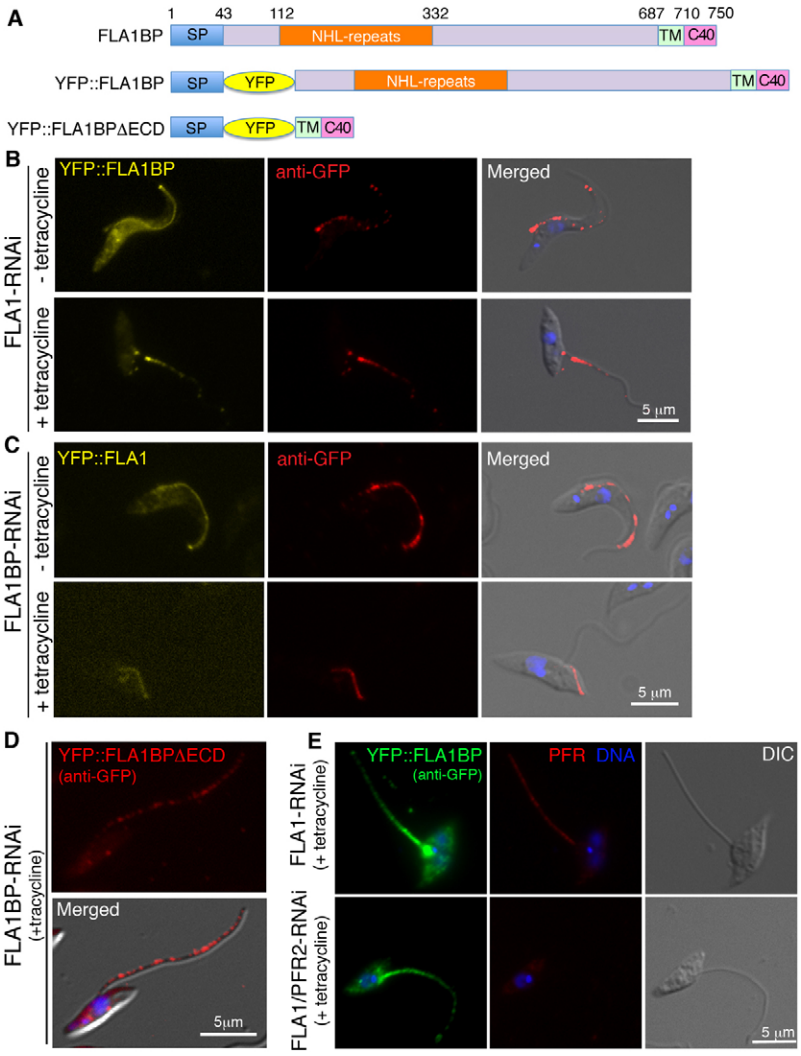

Fig. 4. FLA1BP is a flagellum membrane protein and its localization is independent of the extracellular domain. (**A**) A schematic view of the domain organization of FLA1BP and YFP fusions. Similar to FLA1, FLA1BP contains an N-terminal signal peptide (SP) followed with an NHL-repeat-containing domain, a transmembrane domain and a 40-amino-acid tail. To generate YFP fusions, the YFP was inserted immediately downstream of the signal peptide. (**B**) YFP::FLA1BP was stably expressed in FLA1-RNAi cells cultured in the presence or absence of tetracycline to induce RNAi or not. Surface labeling was performed on cells fixed with 4% PFA, and was examined using methods as described in the Materials and Methods. In uninduced cells, YFP::FLA1BP was detected along the flagellum adhesion region, whereas in FLA1-depleted cells, YFP::FLA1BP was detected on the surface of the detached flagellum by anti-GFP labeling. (**C**) YFP::FLA1 was transiently expressed in FLA1BP-RNAi cells induced with tetracycline or not. Surface immunofluorescence staining with anti-GFP antibody showed YFP::FLA1 localization to the flagellum adhesion region in un-induced cells. In cells depleted of FLA1BP, YFP::FLA1 was present on the cell surface, probably along the FAZ (cf. Fig. 2). Images shown are representative of all transfected cells expressing detectable levels of YFP. (**D**) YFP::FLA1BPΔECD, which did not contain the region used for FLA1BP-RNAi and therefore resistant to RNAi depletion, was transiently expressed in FLA1BP-depleted cells. Anti-GFP labeling revealed its localization primarily to the flagellum. (**E**) The presence of a PFR is not required for FLA1BP localization to the flagellum. YFP::FLA1BP was expressed in cells depleted of both FLA1 and PFR2. Cells were fixed with 4% PFA followed with cold methanol, and stained with anti-GFP to monitor YFP::FLA1BP (green), anti-PAR for PFR (red) and DAPI for DNA (blue). FLA1-RNAi cells stably expressing YFP::FLA1BP were used as control.

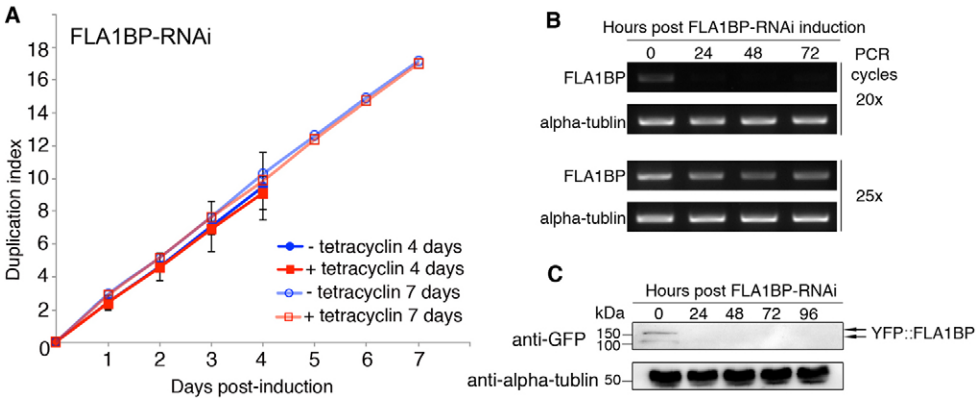

Fig. 5. FLA1BP is not essential for procyclic cell survival in culture. (**A**,**B**) Cells with a stably integrated FLA1BP-RNAi construct were grown in the absence or presence of tetracycline to induce RNAi, and samples were taken every 24 hours for growth analyses (A), and RT-PCR analysis for FLA1BP mRNA levels (B). FLA1BP-depleted cells duplicated at a similar rate to the un-induced control even after 7 days. (**C**) To monitor FLA1BP protein depletion, YFP::FLA1BP was stably expressed in FLA1BP-RNAi cells. The degradation of YFP::FLA1BP was monitored using anti-GFP every 24 hours over the course of RNAi induction. Note that two specific bands were labeled with anti-GFP in YFP::FLA1BP-expressing cells. Both bands could be immunoprecipitated with anti-GFP (see supplementary material Fig. S4) and depletion of both bands was observed upon expression of FLA1BP-RNAi.

using anti-GFP. Despite efficient FLA1BP depletion, the FLA1BP-RNAi cells did not show obvious defects in proliferation rate. Cells lacking FLA1BP continued to duplicate at a rate similar to the un-induced control even 7 days post-induction (Fig. 5A). However, FLA1BP-RNAi cells exhibited drastic changes in morphology. Flagellum detached from cell body in >90% of the cells observed at 2 days post-induction (cf. Fig. 6), supporting the role of FLA1BP in flagellum adhesion.

Flagellum adhesion proteins are required for the coordinated assembly of the flagellum and FAZ

In addition to flagellum detachment, FLA1BP-depleted cells also showed drastic morphological changes in organelle positioning and cell length, which were likely due to disruption of the coordinated flagellum/FAZ assembly (Fig. 6A,B). To test this, we analyzed FLA1BP-depleted cells that contained a single nucleus, a single kinetoplast and a single flagellum, which represented ~60% of the asynchronous population at 7 days post-induction. Detailed measurements of PFR length (an indicator of flagellum length), FAZ length and nucleus/kinetoplast positioning relative to the posterior and anterior tips of the parasite cells were summarized in Fig. 6C. The flagellum, despite being detached from the cell body, measured at 14.3±2.3 μm in FLA1BP-RNAi cells, similar to that of the control cells (13.7±1.9 μm). Whereas in control cells, the flagellum length and FAZ length are strongly correlated (R^2=0.75), this correlation was completely abolished in FLA1BP-RNAi cells (R^2=0.21; Fig. 6D). The FAZ length reduced drastically from 12.1±2.1 μm in control cells to 5.8±1.6 μm in FLA1BP-ablated cells.

Short FAZ led to short cell length. The distance between the nucleus and the posterior end of the cell was 6.3±1.8 μm, decreased only slightly than that in control cells (7.1±1.4 μm; Fig. 6C). The distance between the nucleus and the anterior tip of the parasite (anterior region marked by the presence of the FAZ), however, is shortened from 9.2±1.7 μm in control cells to 6.6±1.5 μm in FLA1BP-RNAi cells (Fig. 6C), suggesting that shortening of the cell body was mainly due to shortening in the anterior region of the parasites. On the other hand, the distance from the kinetoplast and associated basal bodies to the posterior tip, significantly increased from 4.5±1.0 μm to 6.8±1.6 μm (Fig. 6C), thus resulting in the kinetoplast located slightly anterior to the nucleus in FLA1BP-RNAi cells (see Fig. 6A).

Despite the short length, the FAZ appeared normally assembled in FLA1BP-RNAi cells. In addition to the FAZ markers CC2D and FAZ1 (Fig. 6A; supplementary material Fig. S5), YFP::FLA1 was also properly localized to the FAZ region on the cell body side (Fig. 4C). Restoring FLA1BP expression in FLA1BP-RNAi cells by tetracycline removal restored flagellum adhesion, correlation between flagellum length and FAZ length, as well as normal cell morphology (Fig. 6A–D).

To further understand how FLA1BP-RNAi cells divided with a short FAZ, major cell cycle events including the duplication and segregation of nucleus, basal bodies and associated kinetoplast, as well as the assembly of new FAZ and new flagellum were examined in FLA1BP-RNAi cells throughout the cell cycle (Fig. 7). In both control and FLA1BP-RNAi cells, the order and timing of each cell cycle event remained largely unaltered. This was consistent with the observation that FLA1BP-RNAi cell proliferated at the same rate as the control cells and no significant change in cell cycle duration was observed (cf. Fig. 5A). Whereas the new flagellum was assembled along the old flagellum, with its distal tip attached to the old flagellum via the FC, the new FAZ also extended along the old FAZ, with it distal tip attached to the old structure, in both control and FLA1BP-RNAi cells (Fig. 7A,B). However, unlike in control cells where new FAZ and new flagellum assembled in a highly coordinated fashion (R^2=0.92), elongation of the new FAZ was slowed and uncoupled from new flagellum elongation in FLA1BP-RNAi cells (R^2=0.35; Fig. 7C). The short FAZ could also account for the inhibited basal body/kinetoplast segregation observed in these parasites (Fig. 7D), hence the change in kinetoplast positioning in daughter cells (cf. Fig. 6C). Nuclear division, however, was only moderately affected by the short FAZ (Fig. 7E).

Flagellum adhesion proteins mediate flagellum regulation of FAZ length

Lithium chloride treatment has been shown to lengthen flagellum/cilium in *Chlamydomonas reinhardtii* and some mammalian cells (Miyoshi et al., 2009; Wilson and Lefebvre, 2004), by inhibition of

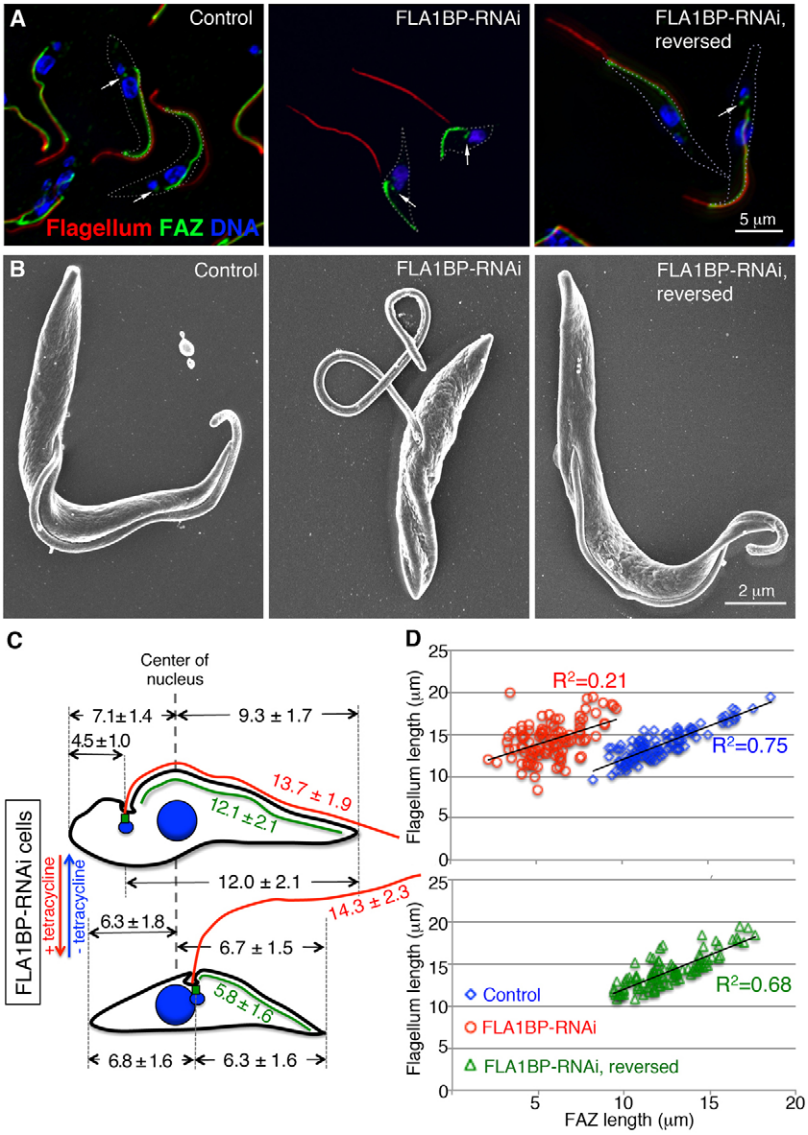

Fig. 6. The expression of FLA1BP is crucial for flagellum adhesion and cell morphology. FLA1BP-RNAi cells were induced with tetracycline for 7 days and followed by tetracycline wash off and continuous culture in tetracycline-free medium for 48 hours. (**A**,**B**) Un-induced control, FLA1BP-RNAi and FLA1BP-RNAi-reversed cells were fixed for immunostaining (A) or scanning electron microscopy (B). For A the cells were fixed with cold methanol and labeled with anti-CC2D for basal bodies (arrows) and FAZ (green), anti-PAR for the paraflagellar rod that was present along most of the extracellular flagellum (red) and DAPI for DNA (blue). Two cells in each panel are demarcated by white dotted lines. (**C**) Un-induced (n=109 cells), FLA1BP-RNAi (n=99 cells) and FLA1BP-RNAi reversed cells (n=100 cells) containing a single nucleus (large blue circle), kinetoplast (small blue circle), flagellum (red line) and FAZ (green line), were quantified for flagellum length, FAZ length, distance between the posterior or anterior tip of the cell to the kinetoplast and associated basal bodies (small green dot), and distance between the posterior or anterior tip of the cell to the center of the nucleus. All values are distance or length measurements in μm. (**D**) In un-induced control cells, the FAZ length was strongly correlated to flagellum length (R^2=0.75, blue). This correlation was disrupted in FLA1BP-RNAi cells (R^2=0.21, red), and mostly restored once FLA1BP-RNAi was reversed (R^2=0.68, green).

the glycogen synthase kinase 3 (GSK3). To confirm that flagellum adhesion proteins play an active role in linking FAZ assembly to flagellum elongation, *T. brucei* cells induced with FLA1BP-RNAi or not were cultured in the presence or absence of 5 mM LiCl for 24 hours, which showed little inhibitory effects on parasite proliferation (Fig. 8A). Flagellum and FAZ lengths were then measured in cells containing one nucleus, one kinetoplast and one flagellum, as described in Fig. 6. The LiCl treatment resulted in a significant increase of flagellum length in both control and FLA1BP-RNAi cells (Fig. 8B,C, P<0.0001). Significant FAZ length increase, however, was only observed in control cells where flagellum adhesion was intact (Fig. 8B, P<0.0001). Cells lacking FLA1BP did not show difference in FAZ length (Fig. 8C, P=0.35), supporting an essential role of flagellum membrane adhesion in transmitting flagellum length information to the intracellular FAZ.

Discussion

Using a FLA1-truncation mutant that lacked the C-terminal 16 amino acids and mislocalized to the flagellum membrane, we isolated a novel FLA1BP, which is the first FLA1-binding protein identified to date. Despite the lack of similarity in amino acid sequences, FLA1BP and FLA1 have similar domain organization: both are transmembrane proteins with extracellular, NHL-repeat-containing domains and short cytoplasmic tails. Further analyses of YFP-tagged FLA1 and FLA1BP in cells with detached flagella, revealed a distinct localization of FLA1BP to the flagellum membrane and FLA1 to the cell membrane along the FAZ. Co-immunoprecipitation confirmed the interaction between FLA1 and FLA1BP, probably through their extracellular domains. A model of their interaction and how this interaction mediates flagellum–cell adhesion is proposed in Fig. 9. In this model, FLA1 spans the cell membrane along the FAZ with its C-terminal 16 amino acids in the cell lumen, possibly playing a role in intracellular FAZ assembly (LaCount et al., 2002). FLA1BP, on the other hand, spans the flagellar membrane, with the C-terminal 40 amino acids facing flagellum lumen and possibly anchored to flagellar axoneme. FLA1 and FLA1BP interact through their extracellular domains, hence linking the flagellum membrane to cell membrane.

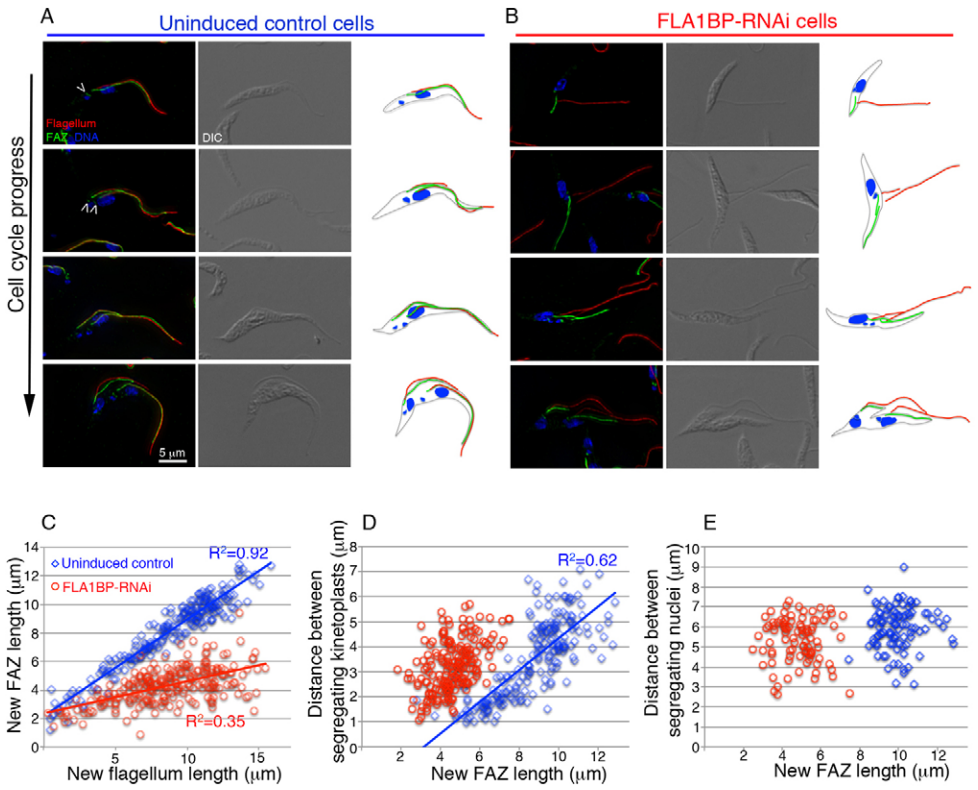

Fig. 7. Flagellum adhesion is essential for coordinated flagellum/FAZ assembly. (**A**,**B**) The cell cycle of control and FLA1BP-RNAi cells. FLA1BP-RNAi cells cultured in the absence or presence of tetracycline for 72 hours were fixed and immunolabeled with anti-CC2D for basal bodies and FAZ (green), PAR for flagellum (red) and DAPI for DNA (blue). In un-induced control cells (A), following duplication of the basal bodies (carets), a new flagellum and a new FAZ were assembled posterior to the old structures. The coordinated elongation of the new flagellum and new FAZ was accompanied by the duplication and segregation of the kinetoplasts (small blue dots) and the nuclei (large blue dots). Images are presented in the order of cell cycle progress based on the number of kinetoplast, nucleus, FAZ and flagellum. These major organelles in each cell were also traced and shown on the right of each panel. In FLA1BP-depleted cells (B), a new, detached flagellum was assembled next to the old flagellum. Though both flagella were detached, the distal tip of the new flagellum remained associated with the old flagellum and elongated along with it, probably through the intact FC. A new FAZ was assembled posterior to the old FAZ structure, also with its distal tip attached to the old structure. (**C**–**E**) The length of the new FAZ and new flagellum, together with the distances between segregating kinetoplasts/basal bodies and dividing nuclei were measured in cells containing two flagella (C), two kinetoplasts (D) or two nuclei (E). Whereas in the uninduced control cells, flagellum and FAZ elongated coordinately with R^2=0.92; in the FLA1BP-RNAi cells, the FAZ assembly slowed, and was not coordinated with flagellum elongation (R^2=0.35). Although kinetoplast segregation was significantly inhibited and not coordinated with FAZ elongation, the segregation of the nuclei was only moderately inhibited in FLA1BP-RNAi cells.

Coordinated flagellum/FAZ assembly requires flagellum/cell membrane adhesion

In *T. brucei*, the flagellum is a multifunctional organelle. In addition to motility and sensory functions, it also regulates cell morphogenesis (Vaughan, 2010). This latter function is via the coordinated assembly of flagellum with the FAZ, which is an intracellular complex important for cell division, organelle segregation and subpellicular microtubule organization (LaCount et al., 2002; Robinson et al., 1995; Vaughan et al., 2008; Zhou et al., 2011). Further dissection of the exact mechanisms of the coordinated assembly required molecular characterization of the flagellum membrane attachment structures.

The identification of FLA1BP, an interacting partner of FLA1, provided the molecular basis of flagellum membrane adhesion to the cell membrane. In cells lacking FLA1BP and flagellum adhesion, the coordinated flagellum/FAZ assembly was disrupted, during both cell cycle development and LiCl treatment. Although the new flagellum formed normally, the FAZ was assembled at a slower rate, to a short but relatively fixed length (5.8±1.6 μm), as indicated by different FAZ markers. This short FAZ was ~50% of the average FAZ length observed in control cells (12.1±2.1 μm). It is not clear if this partial assembly was due to incomplete depletion of FLA1BP, or the presence of other FLA1-related proteins (see below), or an intrinsic length regulation of core FAZ components. However, it appeared that a ~6 μm FAZ was sufficient to support organelle segregation, cell division and cell survival, at least in culture.

The short FAZ is responsible for the shortened cell length, particularly in the anterior region, suggesting that the subpellicular microtubules in the posterior region may be regulated differently to the subpellicular microtubules in the anterior region. The short FAZ was also responsible for the limited segregation of the kinetoplasts and associated basal bodies, but had only moderate effect on the proper segregation of the nuclei.

Reversing FLA1BP-RNAi by removing tetracycline restored flagellum–cell adhesion and the coordinated flagellum–FAZ

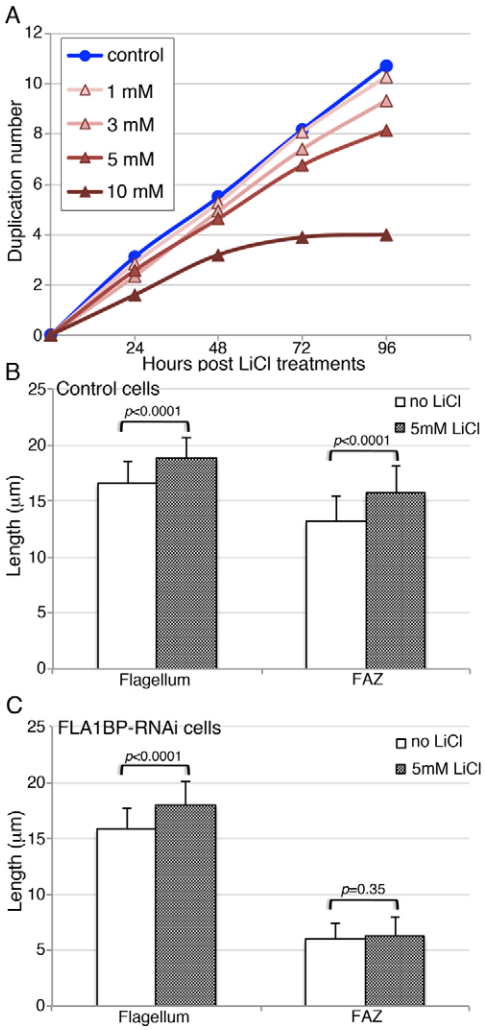

Fig. 8. FLA1BP is required for coordinated flagellum/FAZ growth in LiCl treatments. (**A**) Treatment with up to 5 mM LiCl had little effect on parasite proliferation. *T. brucei* cells were cultured in the presence of 1, 3, 5 and 10 mM LiCl, and the cell proliferation was monitored every 24 hours over 4 days. (**B**) In control parasites, both flagellum and FAZ lengths increased significantly after 24 hours treatment with LiCl ($n=100$ cells that contained one flagellum). (**C**) In cells lacking FLA1BP and flagellum adhesion, the flagellum length increased significantly as in control cells whereas the FAZ length remained short.

assembly, thus allowing the length information contained in the flagellum to be efficiently transmitted to the cell body and thus restoring normal cell morphology. Previous work on GP72 in *T. cruzi* produced similar results in cell morphology (Cooper et al., 1993). Together, these results supported a conserved function of the FLA1-related membrane adhesion proteins in linking flagellum biogenesis to FAZ elongation, therefore regulating cell morphogenesis in trypanosomes.

Flagellum membrane adhesion, an intracellular membrane junction

To understand how the molecular interaction between FLA1 and FLA1BP coordinates flagellum/FAZ assembly, we investigated the targeting of FLA1 and FLA1BP to the flagellum adhesion region. Our present studies indicated that the extracellular domains of FLA1 and FLA1BP were dispensable for their respective localization to the FAZ and the flagellum membrane. The correct targeting of FLA1 and FLA1BP was likely mediated by their short, C-terminal cytoplasmic tails, through specific interaction with other proteins in the cell body or in the flagellum. The C-terminal 16 amino acids of FLA1 has been implicated in directing FAZ assembly (LaCount et al., 2002) and depletion of FLA1 led to inhibited FAZ formation (Vaughan et al., 2008). The C-terminal 40 amino acids of FLA1BP resided in the flagellum lumen and may be associated with flagellum proteins that led to the dotted pattern observed with YFP::FLA1BPΔECD. Whereas FLA1BP-depleted cells were able to proliferate in culture, FLA1 is an essential protein possibly as an integral component of FAZ (Rotureau et al., 2011). Interestingly, the PFR was not essential for YFP::FLA1BP localization to the flagellum in a dotted line, suggesting that FLA1BP may be associated with other structural component, possibly the flagellum axoneme. This is also consistent with the normal flagellum attachment and lack of morphological changes observed in snl-1 cells lacking PFR (Bastin et al., 1998). The FLA1–FLA1BP interaction, and their respective interactions with flagellum axoneme and FAZ proteins, may direct the formation of the membrane–cytoskeleton nexus at flagellum attachment region and thus mediate the highly coordinated flagellum/FAZ assembly during the cell cycle.

The adhesion between the flagellum membrane and the cell membrane (Fig. 9) is reminiscent of cell–cell membrane adhesions observed in multicellular animals, such as the adherens junctions (Yonemura, 2011). The interaction between FLA1 and FLA1BP and their possible association with cytoskeletal components (see Fig. 9), is also similar to cadherins that are transmembrane glycoproteins forming dimers with the extracellular domains and interacting with actin cytoskeleton on the cytoplasmic side. Adherens junctions are important for tissue morphogenesis and signal transduction between linked cells. Given that sensory functions have become increasingly evident in trypanosome flagella, whether FLA1 and FLA1BP also function in signal transduction between the flagellum and cell body will be of great interest.

The FLA1-related proteins

In *T. brucei* database, four additional genes were predicted to encode proteins containing transmembrane domains and NHL repeats arranged in similar fashion as FLA1 and FLA1BP (Table 1). Among them, the amino acid sequences of FLA2 (encoded by Tb927.8.4060) and FLA3 (encoded by Tb927.8.4110) are >97% identical, and each exhibits ~60% identity and 70% similarity, respectively, to FLA1. While FLA1BP (encoded by Tb927.8.4050 and Tb927.8.4100) shows little similarity to FLA1, a FLA1BP-like protein (encoded by Tb927.5.4570 and Tb927.5.4580) was found in the database, showing 40.5% identity and 54.9% similarity to FLA1BP. A sixth FLA1-like protein is encoded by Tb927.10.6180, which shows no homology to either FLA1 or FLA1BP. Interestingly, all FLA1 related proteins with the exception of Tb927.10.6180 appear to be developmentally regulated. While FLA1 and FLA1BP appeared more abundant in the procyclic cells, FLA2/3 and FLA1BP-like protein were more abundant in blood stream form parasites by transcriptome and mRNA expression analyses (Kabani et al., 2009; Queiroz et al., 2009). Owing to the sequence similarity between FLA1 and FLA2/3, and FLA1BP and

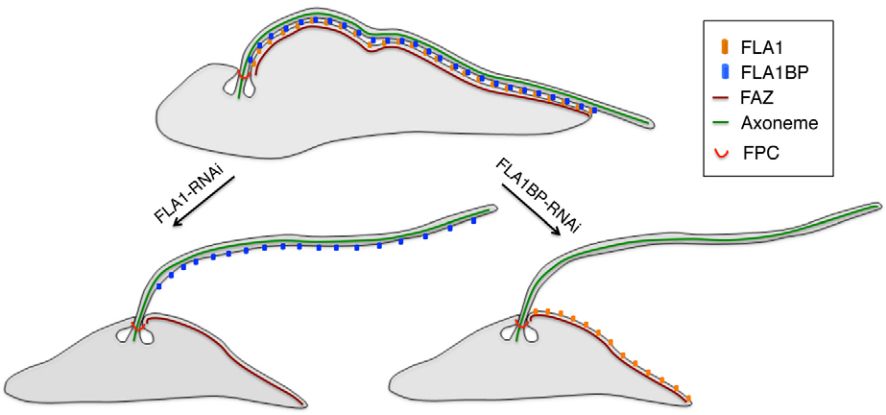

Fig. 9. A model of flagellum adhesion mediated by the interaction of FLA1 and FLA1BP. In *T. brucei*, the flagellum exits the cells body from the cup-shaped flagellar pocket and the flagellum membrane is partitioned from the cell membrane by the flagellar pocket collar (FPC). Upon exit from the cell body, the flagellum membrane adheres to the cell membrane. Both FLA1 and FLA1BP are essential for this adhesion. In this model, FLA1 is present on the cell membrane and FLA1BP is present on the flagellum membrane. FLA1 and FLA1BP interact through the extracellular domains, thus mediating flagellum membrane adhesion. The cytoplasmic tails of FLA1 and FLA1BP may interact with the FAZ and flagellum axoneme, respectively, thus coordinating the assembly of the flagellum–FAZ complex. In the absence of either FLA1 or FLA1BP, the flagellum is detached from the cell body, uncoupling FAZ assembly from flagellum elongation.

FLA1BP-like proteins, it is tempting to speculate that whereas FLA1–FLA1BP interaction mediates flagellum–cell membrane adhesion in procyclic cells, FLA2/3 may interact with FLA1BP-like protein in BSF parasites. Previous studies suggested significant FAZ remodeling during parasite development in tsetse flies (Rotureau et al., 2011). The presence of six FLA1-related proteins, with similar domain organization but distinct sequences and developmental specificity, substantiates the remarkable complexity of the flagellum–cell membrane adhesion during development.

Orthologs to most of the FLA1-related proteins are also found in other kinetoplastid parasites including *T. cruzi* and *Leishmania* spp. (Table 1). Each *T. cruzi* cell contains an attached flagellum similar to *T. brucei*. Flagella in *Leishmania* parasites, however, are only partially attached with a short FAZ (Weise et al., 2000). This unique intracellular membrane adherence junction in a unicellular parasite represents a fascinating opportunity to study signal transduction from flagellum to cell body. The possible specific interaction between two non-variant surface proteins that is not essential for normal cell functions also opens up new ways to combat these lethal human pathogens.

Materials and Methods

Cell culture

Procyclic form YTat1.1 cell line (Ruben et al., 1983) was cultured in Cunningham's medium supplemented with 15% heat-inactivated fetal bovine serum (Hyclone) at 28℃. Procyclic form 29.13 cell line engineered for tetracycline-inducible expression (Wirtz et al., 1999) was maintained in Cunningham's medium supplemented with 15% heat-inactivated, tetracycline-free fetal bovine serum (Clontech) in the presence of 15 μg/ml G418 and 50 μg/ml hygromycin at 28℃.

Plasmid construction and transfection methods

For FLA1-RNAi, a 302-bp fragment (nucleotides 715–1016) or a 390-bp fragment of FLA1 (nucleotides 1364–1641 of the coding sequence and 112 nucleotides in 3′-untranslated region) was PCR amplified and cloned into a pZJM construct (Wang et al., 2000) with blasticidin resistance, which allows tetracycline-inducible RNAi. Both RNAi constructs produced inhibitory effects on cell growth and flagellum attachment, similar to the RNAi phenotypes previously observed with a 1006-bp fragment of FLA1 (nucleotides 64–1070) (LaCount et al., 2002) (supplementary material Fig. S2; Fig. 2A; Fig. 4B). RNAi cell line created with the 302-bp fragment was used for the expression of FLA1-RNAi resistant mutant YFP::FLA1ΔECD; RNAi cell line created with the 389-bp fragment was used for the expression of RNAi-resistant YFP::FLA1ΔC16^{R} (see below). For FLA1BP-RNAi, a 518-bp fragment within FLA1BP coding sequence (nucleotides1385–1902) was PCR-amplified and cloned into pZJM with blasticidin-resistance marker.

A pXS2/YFP vector (Bangs et al., 1996; He et al., 2004) was used for stable and transient expression of YFP-tagged proteins. The N-terminal 99-bp of FLA1, which codes for the signal peptide was PCR-amplified from *T. brucei* genomic DNA with primers 5′-CCCAAGCTTATGGGTGGCAGGACTGAATCACGGG-3′ (*Hin*dIII site underlined) and 5′-CTAGCTAGCGGTTTGGTCTCCTATAACGGGACTC-3′ (*Nhe*I site underlined), digested with *Hin*dIII and *Nhe*I, and fused to the N-terminus of YFP in pXS2/YFP; the remaining 1542-bp coding region of FLA1 (nucleotides 100–1641) was then PCR-amplified with primers 5′-GA-AGATCTGTGGGCACCAAGGTGATTGTGAACC-3′ and 5′-GAAGATCTTTA-TCACTCGAACGCCGGCAACCGTACA-3′ (*Bgl*II sites underlined), digested with *Bgl*II and fused to the C-terminus of YFP, thus producing the pXS2/YFP::FLA1 construct. The FLA1ΔECD truncation mutant (containing nucleotides 1516–1641 of FLA1 coding sequence) was PCR-amplified with primers 5′-CG-GGATCCGTGTGTCTCGGTGGTATCGTTTCCTC-3′ (*Bam*HI site underlined) and 5′-CGGAATTCTCACTCGAACGCCGGCAA-3′ (*Eco*RI site underlined), digested with *Bam*HI and *Eco*RI, and fused into the C-terminus of FLA1 signal peptide and YFP, producing the YFP::FLA1ΔECD. Using YFP::FLA1 or YFP:FLA1ΔECD as a template, a stop codon TGA was introduced after the transmembrane domain (nucleotides 1519–1590) with primers 5′-TTTCCTG-ATGGTGGTATGAAGCCCGTACAACGTAA-3′ and 5′-TTACGTTGTACGG-GCTTCATACCACCATCAGGA AA-3′ (stop codons underlined), thus producing YFP::FLA1ΔC16 and YFP::FLA1TM, respectively. YFP::FLA1ΔC16RR was constructed by placing two genetic codons for arginine (R) and a stop codon immediately after the transmembrane domain (nucleotides 1519–1590) through PCR amplification with primers 5′-GAAGATCTTCACCGACGTACCACCATCAG-3′ (stop codon underlined and genetic codon of arginine under dotted line). To construct RNAi-resistant FLA1 truncation mutants, nucleotides 1360–1590 of FLA1 with scramble codons (supplementary material Fig. S3A), was synthesized and used to replace all corresponding regions in the FLA1 mutants. For tetracycline inducible expression, the YFP-tagged FLA1 mutants were cloned into the plew100 vector with phleomycin resistance (Wirtz et al., 1999). Proper expression of the RNAi-resistant YFP::FLA1ΔC16^{R} was verified by immunoblots with anti-FLA1 and anti-GFP, respectively (supplementary material Fig. S3B).

For expression of FLA1BP as YFP fusions, the N-terminal 135 nucleotides that contained the N-terminal transmembrane domain was PCR amplified with primers 5′-CCCAAGCTTATGCCGTTGTGGAAACAAACC-3′ (*Hin*dIII site underlined) and 5′-CTAGCTAGCACTCTCACTACAATCGTTGCG-3′ (*Nhe*I site underlined), digested with *Hin*dIII and NheI, and fused to the N-terminus of YFP in a pHD1034 vector with puromycin resistance (Quijada et al., 2002); the rest of FLA1BP coding sequence (nucleotides 136–2253) was then PCR-amplified with primers 5′-CGGGATCCGGAGCCGCTCCCATTGAA-3′ (*Bam*HI site underlined) and 5′-GGAATTCTCACTGCTCGACCCTTTCTTT-3′ (*Eco*RI site underlined), and fused to the C-terminus of YFP, thus generating YFP::FLA1BP. Alternatively, FLA1BP coding sequence containing only the C-terminal transmembrane domain and 40-amino-acid tail (nucleotides 2059–2250) was PCR amplified with primers 5′-CGGGATCCCGCGTGTGCCTAATCATAATC-3′

(*Bam*HI site underlined) and 5′-GGAATTCTCACTGCTCGACCCTTTCTTT-3′ (*Eco*RI site underlined), and engineered to the C-terminus of YFP to generate YFP::FLA1BPΔECD.

For transient transfections, 50 µg of plasmid DNA was introduced into parasites by electroporation. Transient expression of YFP fusions was monitored typically at 16 hours post-transfection. For stable transfections, 15 µg linearized plasmid DNA was used for electroporation, and stable clones selected by appropriate antibiotics and serial dilution.

RT-PCR

Total RNA was isolated from 5×10^7 cells using Trizol® reagent (Invitrogen, USA). Isolated RNA was treated with RNase-free DNase I (Roche, Germany) and the first-strand cDNA was synthesized using M-MLV reverse transcriptase (Invitrogen, USA) with oligo(dT)12–18 primer (Fermentas, USA). The cDNA level of FLA1BP was then monitored by PCR amplification of a 202 base pairs fragment with primers 5′-CGGGATCCCGCGTGTGCCTAATCATAATC-3′ and 5′-GGAATTCTCACTGCTCGACCCTTTCTTT-3′ using varying PCR cycles. As a control, the cDNA level of α-tubulin was monitored by PCR amplification of a 164-bp fragment with primers 5′-AAGCGCGCCTTCGTGCACTG-3′ and 5′-CGGGATCCCTAGTACTCCTCCACATCCTCC-3′.

Growth assay

Log-phase cells were diluted to 2×10^5 cells/ml to initiate a growth assay. Cell densities were measured every 24 hours by a hemocytometer. If cell density exceeded 10^6 cells/ml, the culture was diluted with fresh medium to 10^6 cells/ml to avoid overgrowth in the next 24-hour period. Duplication index was calculated as $\mathrm{Log}_2\,(N_t\times Df/N_0)$, where Df is the dilution factor, N_t is cell density at each time point and N_0 is the cell density at $t=0$.

Co-immunoprecipitation

Cells with stably transfected pLew100/YFP:FLA1ΔC16^R and pZJM/FLA1 were cultured in the presence of 10 µg/ml tetracycline for 40 hours to induce FLA1-RNAi and expression of YFP::FLA1ΔC16^R. Approximately 4×10^9 cells were harvested, washed with pre-chilled gPBS (phosphate-buffered saline containing 1 g/l glucose), and resuspended with cold gPBS containing 1.5 mg/ml biotin (Pierce 21335). Surface biotinylation was carried out on ice for 30 minutes, and 2 M Tris buffer (pH 6.8) was added to 100 mM final concentration to terminate biotinylation. Parasite cells were washed twice, resuspended in 1 ml gPBS containing 100 mM Tris and protein inhibitors (5 µg/ml pepstain, 5 µg/ml leupeptin, 1 µM PMSFs and 5 µg/ml aprotinin; Sigma), and lysed by brief sonication. Triton X-100 was then added the cell lysate to 1% and the cells were extracted at 4℃ for 1 hour with gentle mixing. After centrifugation at 20,000 g for 30 minutes at 4℃, the cleared cell lysate was incubated with 50 µl anti-GFP bound Dynabeads (Invitrogen) at 4℃ overnight. The Dynabeads were washed twice with PBS containing 1% Triton X-100, 100 mM Tris and protein inhibitors, and twice with PBS containing 100 mM Tris. For elution of proteins bound to anti-GFP, the Dynabeads were incubated with 200 µl 200 mM glycine (pH 1.8) for 3 minutes and the eluate rapidly neutralized with Tris buffer (pH 10). 40 µl streptavidin beads (Invitrogen) were then incubated with the neutralized eluate. After the incubation, the beads were washed three times in buffer containing 8 M urea, 1% SDS and 100 mM Tris, pH 8. Proteins bound to the streptavidin beads were eluted by boiling in the presence of gel loading buffer containing 1% SDS and 11.9 mM β-mecaptoethanol and fractionated on 10% SDS-PAGE. The gels were then further processed for silver staining, mass spectrometry (MS) and immunoblotting.

LC-MS/MS analysis

Each dried peptide was reconstituted in 3% acetonitrile and 0.1% formic acid and analyzed by an LTQ-FT ultra mass spectrometer (ThermoFisher Scientific) and a Prominence™ HPLC unit (Shimadzu). The peptide samples were injected, concentrated and subsequently resolved in a capillary column (200 µm ID×10 cm). Mobile phase buffer A (0.1% formic acid in H_2O) and buffer B (0.1% formic acid in acetonitrile) were used to establish the 60-minute gradient before re-equilibration of the column. HPLC was performed at a constant flow rate of 20 µl/min, and ~300 nl/min at the electrospray emitter (Michrom BioResources). Under an electrospray potential of 1.5 kV, samples were ionized in an ADVANCE™ CaptiveSpray™ Source (Michrom BioResources). Data acquired by LTQ-FT ultra in the positive ion mode was used to perform a full MS scan at a resolution of 100,000 and a maximum ion accumulation time of 1000 ms. To collect peptides and measure peptide fragments by collision-induced dissociation, a linear ion trap was used with the AGC setting. All MS/MS spectra were searched against *Trypanosoma brucei* GeneDB (Berriman et al., 2005) for protein identification using Mascot (version 2.2.07, Matrix Science, Boston, MA, USA) search engines.

Fluorescence microscopy

Unless otherwise stated, cells were attached to coverslips, fixed and permeabilized in methanol at −20℃ for 10 minutes and blocked with 3% BSA in PBS for 1 hour before immunolabeling. For surface labeling with the anti-GFP antibody, live cells were incubated with antibodies on ice (Haynes et al., 1996), fixed *in situ* with 2 or 4% EM grade paraformadehyde (PFA) and then observed under microscope. Alternatively, cells were fixed *in situ* with 2 or 4% EM grade PFA for 20 minutes. Fixed but non-permeabilized cells were then probed with antibodies and processed for microscopy. Membrane permeabilization under these conditions was not detected using cells expressing YFP only (cf. Fig. 1G). The antibodies anti-PAR (1:2000), L3B2 (1:25) or anti-CC2D (1:500) were used to label the paraflagellar rod, FAZ 1 in the FAZ filament, and CC2D at the FAZ, respectively. Images (single slices or z-stacks) were acquired by a Zeiss Axio Observer Z1 fluorescence microscope equipped with a 63× NA 1.4 objective and a CoolSNAP HQ2 CC2D camera (Photometrics). Z-stack images were collected at 0.3–0.5 µm steps, deconvolved and projected as 2D images. Image processing was performed with AxioVision Rel. 4.8 (for deconvolution), ImageJ (for length/distance measurements) and Photoshop CS extended version 12.0 (for figure preparation).

Scanning electron microscopy

For scanning electron microscopy, cells were fixed with 2.5% glutaraldehyde in Cunningham's medium situ for 2 hours and attached to coverslips by centrifugation at 4000 rpm for 10 minutes. Cells were then washed twice with 0.1 M cacodylate buffer (pH 7.4, filtered), one time with distilled water, and post-fixed with 1% O_SO_4 in H_2O for 1 hour at room temperature. After fixation, cells were washed with distilled water once and dehydrated in increasing concentrations of ethanol: 30% ethanol, 50% ethanol, 70% ethanol, 80% ethanol, 90% ethanol, 95% ethanol each for 10 minutes and 100% ethanol twice for 20 minutes. After dehydration, cells were critical point dried, coated with carbon by a vacuum evaporator (JEOL), and viewed using a Helios NanoLab DualBeam electron microscope (FEI).

Acknowledgements

We thank Ms Meng Mei at Nanyang Technological University for assistance with mass spectrometry and Dr Zakayi Pius Kabututu for technical assistance. We also thank Professor George Cross for the Flap2 antibody (anti-FLA1), Professor Keith Gull and Philippe Bastin for the L3B2 antibody, and Professor Diana McMahon-Pratt for anti-PAR.

Funding

The work was supported by the Singapore National Research Foundation [grant number NRF-RF001-121 to C.Y.H.]

Supplementary material available online at
http://jcs.biologists.org/lookup/suppl/doi:10.1242/jcs.113621/-/DC1

References

Absalon, S., Kohl, L., Branche, C., Blisnick, T., Toutirais, G., Rusconi, F., Cosson, J., Bonhivers, M., Robinson, D. and Bastin, P. (2007). Basal body positioning is controlled by flagellum formation in Trypanosoma brucei. *PLoS ONE* **2**, e437.

Bangs, J. D., Brouch, E. M., Ransom, D. M. and Roggy, J. L. (1996). A soluble secretory reporter system in Trypanosoma brucei. Studies on endoplasmic reticulum targeting. *J. Biol. Chem.* **271**, 18387-18393.

Bastin, P., Sherwin, T. and Gull, K. (1998). Paraflagellar rod is vital for trypanosome motility. *Nature* **391**, 548.

Berriman, M., Ghedin, E., Hertz-Fowler, C., Blandin, G., Renauld, H., Bartholomeu, D. C., Lennard, N. J., Caler, E., Hamlin, N. E., Haas, B. et al. (2005). The genome of the African trypanosome Trypanosoma brucei. *Science* **309**, 416-422.

Broadhead, R., Dawe, H. R., Farr, H., Griffiths, S., Hart, S. R., Portman, N., Shaw, M. K., Ginger, M. L., Gaskell, S. J., McKean, P. G. et al. (2006). Flagellar motility is required for the viability of the bloodstream trypanosome. *Nature* **440**, 224-227.

Cooper, R., Inverso, J. A., Espinosa, M., Nogueira, N. and Cross, G. A. (1991). Characterization of a candidate gene for GP72, an insect stage-specific antigen of Trypanosoma cruzi. *Mol. Biochem. Parasitol.* **49**, 45-59.

Cooper, R., de Jesus, A. R. and Cross, G. A. (1993). Deletion of an immunodominant Trypanosoma cruzi surface glycoprotein disrupts flagellum-cell adhesion. *J. Cell Biol.* **122**, 149-156.

Edwards, T. A., Wilkinson, B. D., Wharton, R. P. and Aggarwal, A. K. (2003). Model of the brain tumor-Pumilio translation repressor complex. *Genes Dev.* **17**, 2508-2513.

Engstler, M., Pfohl, T., Herminghaus, S., Boshart, M., Wiegertjes, G., Heddergott, N. and Overath, P. (2007). Hydrodynamic flow-mediated protein sorting on the cell surface of trypanosomes. *Cell* **131**, 505-515.

Gluenz, E., Ginger, M. L. and McKean, P. G. (2010). Flagellum assembly and function during the Leishmania life cycle. *Curr. Opin. Microbiol.* **13**, 473-479.

Haynes, P. A., Russell, D. G. and Cross, G. A. (1996). Subcellular localization of Trypanosoma cruzi glycoprotein Gp72. *J. Cell Sci.* **109**, 2979-2988.

He, C. Y., Ho, H. H., Malsam, J., Chalouni, C., West, C. M., Ullu, E., Toomre, D. and Warren, G. (2004). Golgi duplication in Trypanosoma brucei. *J. Cell Biol.* **165**, 313-321.

Kabani, S., Fenn, K., Ross, A., Ivens, A., Smith, T. K., Ghazal, P. and Matthews, K. (2009). Genome-wide expression profiling of in vivo-derived bloodstream parasite stages and dynamic analysis of mRNA alterations during synchronous differentiation in Trypanosoma brucei. *BMC Genomics* **10**, 427.

Kohl, L., Sherwin, T. and Gull, K. (1999). Assembly of the paraflagellar rod and the flagellum attachment zone complex during the Trypanosoma brucei cell cycle. *J. Eukaryot. Microbiol.* **46**, 105-109.

Kohl, L., Robinson, D. and Bastin, P. (2003). Novel roles for the flagellum in cell morphogenesis and cytokinesis of trypanosomes. *EMBO J.* **22**, 5336-5346.

LaCount, D. J., Barrett, B. and Donelson, J. E. (2002). Trypanosoma brucei FLA1 is required for flagellum attachment and cytokinesis. *J. Biol. Chem.* **277**, 17580-17588.

Mathers, C. D., Ezzati, M. and Lopez, A. D. (2007). Measuring the burden of neglected tropical diseases: the global burden of disease framework. *PLoS Negl. Trop. Dis.* **1**, e114.

Miyoshi, K., Kasahara, K., Miyazaki, I. and Asanuma, M. (2009). Lithium treatment elongates primary cilia in the mouse brain and in cultured cells. *Biochem. Biophys. Res. Commun.* **388**, 757-762.

Moreira-Leite, F. F., Sherwin, T., Kohl, L. and Gull, K. (2001). A trypanosome structure involved in transmitting cytoplasmic information during cell division. *Science* **294**, 610-612.

Nozaki, T., Haynes, P. A. and Cross, G. A. (1996). Characterization of the Trypanosoma brucei homologue of a Trypanosoma cruzi flagellum-adhesion glycoprotein. *Mol. Biochem. Parasitol.* **82**, 245-255.

Oberholzer, M., Langousis, G., Nguyen, H. T., Saada, E. A., Shimogawa, M. M., Jonsson, Z. O., Nguyen, S. M., Wohlschlegel, J. A. and Hill, K. L. (2011). Independent analysis of the flagellum surface and matrix proteomes provides insight into flagellum signaling in mammalian-infectious trypanosoma brucei. *Mol. Cell. Proteomics* **10**, M111.010538.

Ogbadoyi, E. O., Robinson, D. R. and Gull, K. (2003). A high-order trans-membrane structural linkage is responsible for mitochondrial genome positioning and segregation by flagellar basal bodies in trypanosomes. *Mol. Biol. Cell* **14**, 1769-1779.

Queiroz, R., Benz, C., Fellenberg, K., Hoheisel, J. D. and Clayton, C. (2009). Transcriptome analysis of differentiating trypanosomes reveals the existence of multiple post-transcriptional regulons. *BMC Genomics* **10**, 495.

Quijada, L., Guerra-Giraldez, C., Drozdz, M., Hartmann, C., Irmer, H., Ben-Dov, C., Cristodero, M., Ding, M. and Clayton, C. (2002). Expression of the human RNA-binding protein HuR in Trypanosoma brucei increases the abundance of mRNAs containing AU-rich regulatory elements. *Nucleic Acids Res.* **30**, 4414-4424.

Ralston, K. S., Lerner, A. G., Diener, D. R. and Hill, K. L. (2006). Flagellar motility contributes to cytokinesis in Trypanosoma brucei and is modulated by an evolutionarily conserved dynein regulatory system. *Eukaryot. Cell* **5**, 696-711.

Robinson, D. R., Sherwin, T., Ploubidou, A., Byard, E. H. and Gull, K. (1995). Microtubule polarity and dynamics in the control of organelle positioning, segregation, and cytokinesis in the trypanosome cell cycle. *J. Cell Biol.* **128**, 1163-1172.

Rotureau, B., Subota, I. and Bastin, P. (2011). Molecular bases of cytoskeleton plasticity during the Trypanosoma brucei parasite cycle. *Cell. Microbiol.* **13**, 705-716.

Ruben, L., Egwuagu, C. and Patton, C. L. (1983). African trypanosomes contain calmodulin which is distinct from host calmodulin. *Biochim. Biophys. Acta* **758**, 104-113.

Sharma, R., Peacock, L., Gluenz, E., Gull, K., Gibson, W. and Carrington, M. (2008). Asymmetric cell division as a route to reduction in cell length and change in cell morphology in trypanosomes. *Protist* **159**, 137-151.

Sherwin, T. and Gull, K. (1989). The cell division cycle of Trypanosoma brucei brucei: timing of event markers and cytoskeletal modulations. *Philos. Trans. R. Soc. Lond. B Biol. Sci.* **323**, 573-588.

Slack, F. J. and Ruvkun, G. (1998). A novel repeat domain that is often associated with RING finger and B-box motifs. *Trends Biochem. Sci.* **23**, 474-475.

Vaughan, S. (2010). Assembly of the flagellum and its role in cell morphogenesis in Trypanosoma brucei. *Curr. Opin. Microbiol.* **13**, 453-458.

Vaughan, S., Kohl, L., Ngai, I., Wheeler, R. J. and Gull, K. (2008). A repetitive protein essential for the flagellum attachment zone filament structure and function in Trypanosoma brucei. *Protist* **159**, 127-136.

Wang, Z., Morris, J. C., Drew, M. E. and Englund, P. T. (2000). Inhibition of Trypanosoma brucei gene expression by RNA interference using an integratable vector with opposing T7 promoters. *J. Biol. Chem.* **275**, 40174-40179.

Weise, F., Stierhof, Y. D., Kühn, C., Wiese, M. and Overath, P. (2000). Distribution of GPI-anchored proteins in the protozoan parasite Leishmania, based on an improved ultrastructural description using high-pressure frozen cells. *J. Cell Sci.* **113**, 4587-4603.

Wilson, N. F. and Lefebvre, P. A. (2004). Regulation of flagellar assembly by glycogen synthase kinase 3 in Chlamydomonas reinhardtii. *Eukaryot. Cell* **3**, 1307-1319.

Wirtz, E., Leal, S., Ochatt, C. and Cross, G. A. (1999). A tightly regulated inducible expression system for conditional gene knock-outs and dominant-negative genetics in Trypanosoma brucei. *Mol. Biochem. Parasitol.* **99**, 89-101.

Yonemura, S. (2011). Cadherin-actin interactions at adherens junctions. *Curr. Opin. Cell Biol.* **23**, 515-522.

Zhou, Q., Liu, B., Sun, Y. and He, C. Y. (2011). A coiled-coil- and C2-domain-containing protein is required for FAZ assembly and cell morphology in Trypanosoma brucei. *J. Cell Sci.* **124**, 3848-3858.